

SOFT ELECTROMAGNETIC RADIATIONS FROM RELATIVISTIC HEAVY ION COLLISIONS

Dipali Pal, Pradip Kumar Roy, Sourav Sarkar, Dinesh Kumar Srivastava
Variable Energy Cyclotron Centre, 1/AF Bidhan Nagar, Calcutta 700 064

Bikash Sinha
Variable Energy Cyclotron Centre, 1/AF Bidhan Nagar, Calcutta 700 064
Saha Institute of Nuclear Physics, 1/AF Bidhan Nagar, Calcutta 700 064
(June 9, 2021)

The production of low mass dileptons and soft photons from thermalized Quark Gluon Plasma (QGP) and hadronic matter in relativistic heavy ion collisions is evaluated. A boost invariant longitudinal and cylindrically symmetric transverse expansion of the systems created in central collision of lead nuclei at CERN SPS, BNL RHIC, and CERN LHC, and undergoing a first order phase transition to hadronic matter is considered. A large production of low mass ($M < 0.3$ GeV) dileptons, and soft photons ($p_T < 0.4$ GeV) is seen to emanate from the bremsstrahlung of quarks and pions. We find an increase by a factor of 2–4 in the low mass dilepton and soft photon yield as we move from SPS to RHIC energies, and an increase by an order of magnitude as we move from SPS to LHC energies. Most of the soft radiations are found to originate from pion driven processes at SPS and RHIC energies, while at the LHC energies the quark and the pion driven processes contribute by a similar amount. The study of the transverse mass distribution is seen to provide interesting details of the evolution. We also find a unique universal behaviour for the ratio of M^2 weighted transverse mass distribution for $M = 0.1$ GeV to that for $M = 0.2$ and 0.3 GeV, as a function of M_T , for SPS, RHIC, and LHC energies, in the absence of transverse expansion of the system. A deviation from this universal behaviour is seen as a clear indication of the flow.

PACS number(s): 12.38.Mh, 13.40.-f, 13.85.Qk, 25.75.+r

I. INTRODUCTION

Production, detection, and study of quark-gluon plasma (QGP) constitutes one of the most important challenges of present day nuclear physics. There are plausible reasons to believe that this deconfined state of strongly interacting matter may be produced in collisions involving heavy nuclei. This expectation has led to a great deal of excitement, and a number of international collaborative efforts are underway to identify the signatures of QGP. Of these, lepton pairs (e^+e^- or $\mu^+\mu^-$) and photons are considered as one of the more reliable probes of this hot and dense phase since their mean free path is quite large compared to typical nuclear size enabling them to escape without any final state interaction. Their abundance and spectral distributions are also a rapidly

varying function of the temperature and thus they furnish most valuable information about the nascent plasma.

Spurred by these expectations a considerable theoretical effort has been devoted to the study of large mass dileptons and high p_T photons, which may have their origin mostly in the early stages of the QGP. A number of experiments ¹, viz., WA80, WA93, WA98, HELIOS, CERES, and NA38 experiments at the CERN SPS, the PHENIX experiment at the BNL RHIC, and the ALICE experiment at the CERN LHC, are designed towards measuring the electromagnetic radiations from relativistic heavy ion collisions. It should be remembered, though, that photons and dileptons are emitted at every stage of the evolution of the system, and they carry rather more precise imprints of the circumstances of their ‘birth’. We shall see that the intense glow of soft photons and low mass dileptons can provide reliable and useful information about the later stages of the interacting system.

We concentrate in particular on soft photons and low-mass dileptons produced by bremsstrahlung processes whose energies are low enough to enable us to use the so-called soft-photon approximation [1]. This brings in a unique advantage as, but for a ‘known’ phase space factor (see later) arising due to the finite mass of the dileptons, the basic cross-sections for the two processes become identical. The dileptons of different invariant masses, however, are affected differently by the transverse flow, which should be substantial towards the last moments of the interacting system. A comparison of the yield of dileptons of different masses and photons could then provide us with a valuable information about the flow. This identity of the cross-section for the basic process is not available, for example, between single photons originating from Compton and annihilation processes (in the QGP), and nuclear reactions of the type, say, $\pi\rho \rightarrow \pi\gamma$ in the hadronic matter or quark or pion annihilation processes for the dileptons.

¹ Was this the face that launched a thousand ships?
And burnt the topless towers of Ilium?
Sweet Helen, make me immortal with a kiss..
– Faustus, Christopher Marlowe (1564–1593)

It is also important to understand this contribution in quantitative detail as it is quite likely that the lowering of the mass of ρ mesons, due to high baryonic densities reached in such collisions, for example, will populate the mass region well below the m_ρ in case of dileptons. Thus for example, Li et al [2] postulate that the mass of the ‘primordial’ ρ mesons may have dropped to 370 MeV in S+Au collisions at the CERN SPS studied by the CERES group [3]. The drop is likely to be even larger for the Pb+Pb collision at the SPS energies, in their treatment [4]. This increase in the net baryonic density is unlikely to be achieved at the RHIC or the LHC energies because of the considerable increase in the transparency.

On the other hand, there are reasons to believe that the pion-form factor $F_\pi(M)$, as well as the decay width (Γ_ρ) of the ρ meson, e.g., may depend on the temperature, either because of chiral symmetry restoration, or collision broadening, or both. Thus, in the simplest approximation for the chiral perturbation theory, modifications of F_π and $\Gamma(\rho)$ are given by [5]

$$F_\pi(M, T) = F_\pi(M, 0) \left(1 - \frac{T^2}{8F_\pi^2(M, 0)} \right),$$

$$\Gamma_\rho(T) = \Gamma_\rho(0) / \left(1 - \frac{T^2}{4F_\pi^2(M, 0)} \right), \quad (1)$$

with the mass of the ρ meson remaining essentially unchanged (see e.g., Ref. [6] for more recent developments). This corresponds to a decrease in F_π by about 30% and an increase in Γ_ρ by a factor of 3 at $T=160$ MeV, thus affecting the production of dileptons from annihilation of pions beyond $M \approx 400$ MeV or so. The broadening of the $\Gamma(\rho)$ due to collisions has been estimated by Haglin [7] as

$$\Gamma_\rho(T) = \Gamma_\rho(0) + (a + bT + cT^2), \quad (2)$$

where $a = 0.50$ GeV, $b = -7.16$, and $c = 30.16$ GeV⁻¹, and corresponds to an increase of about 80% at $T = 160$ MeV, whose effect will be limited to dileptons from pion annihilation beyond $M \approx 500$ MeV.

Recall that in the early days of the investigations of QGP it was often suggested that thermal dileptons having an invariant mass less than $2m_\pi$ could originate only from the annihilation of quarks and anti-quarks which were assumed to be essentially massless. Very soon it was realized (see Ref. [8,9] and references therein) that there could be substantial production of dileptons having lower invariant masses from the bremsstrahlung of pions as well as quarks. A better understanding [10,11] of the dynamics of hot QCD has endowed quarks with a thermal mass of a few hundred MeV. If we believe [12] that the invariant mass of the dileptons will have $M \geq 2m_{\text{th}}$, if they originate from the quark annihilation, then the mass window below a few hundred MeV is populated primarily by dileptons from bremsstrahlung processes at the colliders. Of course, there would be a background from Dalitz decays of η and π^0 mesons, which will have

to be eliminated before the glow of the soft dileptons becomes visible. Similar considerations will apply to soft photons originating from the bremsstrahlung of pions.

The QGP likely to be produced in relativistic heavy ion collisions will have enormous internal pressure, and will expand rapidly [13]. If the life time of the interacting system is large compared to $\sim R_T/c_s$, where R_T is the transverse size of the system and c_s is the speed of sound, the consequences of the transverse expansion will become very evident. The last stages of the interacting system are also likely to be repository of the details of the flow, and thus the soft photons and low mass dileptons which derive their maximum contributions from this stage will also carry unique information about the flow.

We organise our paper as follows. In Section II we briefly recall the formulation for the bremsstrahlung production of soft photons and low mass dileptons. Section III describes the results and discussions related to various approximations used in the work are given in Section IV. Finally we give a brief Summary. With this we also conclude our study of soft electromagnetic radiations [14,15] initiated earlier.

II. FORMULATION

A. Soft Photon Approximation

The production of low mass dileptons and soft photons is most conveniently evaluated within a soft-photon approximation. In so far as this approximation remains valid, it provides for an easy manipulation of the strong interaction part of the scattering and enables us to test the sensitivity of the results to such details.

Thus the first question which comes to mind is, how reliable is the soft-photon approximation? The existing treatments for the bremsstrahlung production of low mass dileptons were critically examined by Lichard, recently [16]. We shall, as in our earlier works [14,15], use the correct numerical factor of $(\alpha/3\pi M^2)$ in Eq.(8) (see later) and also use the virtual photon current, as suggested by Lichard.

A reasonably accurate check on the soft photon approximation for the quark driven processes can be obtained from a comparison with the rate for a zero-momentum soft dilepton production [17] in a QGP evaluated by using the resummation technique of Braaten and Pisarski [10]. This was done recently [9], with interesting results. To quote, it was found that for dileptons having masses $M \leq 0.1$ GeV, the soft photon approximation gives results which are very close to the findings of QCD perturbation theory. The soft photon approximation was found to lead to results which were smaller by a factor of about 1–4 for $0.1 \leq M \leq 0.3$ GeV. This has its origin in the fact that the QCD perturbation theory includes the annihilation process, which contributes substantially at larger masses (see figs.1a–c, later). This

comparison provides two important insights; viz., scattering with virtual bremsstrahlung (rather than annihilation or Compton-like processes) accounts for most of the low-mass QGP-driven pairs and the soft-photon approximation as applied to quark processes is fairly reasonable. We must add that we shall depict lowest order annihilation process $q\bar{q} \rightarrow e^+e^-$ clearly and separately.

In a recent study, Eggers et al. [18] have evaluated the bremsstrahlung production of dileptons from pion driven processes, without using the soft-photon approximation in a One Boson Exchange model for the interaction of pions. One of the many interesting observations in that work is that the use of the soft-photon approximation in terms of the invariant mass of the dileptons can overestimate the contribution of the bremsstrahlung processes. We use the soft-photon approximation in terms of the four-momenta of the real or the virtual photons, and thus we feel that we are relatively safe from this criticism. Thus we insist that both M and q remain reasonably small. We have also limited ourselves to invariant masses upto 300 MeV. Still it is worthwhile to recall that even though the individual contributions from different reactions involving pions to the basic cross-section ($d\sigma/dM$) are off by differing amounts as compared to the predictions of the soft-photon approximation, the rates are overestimated by atmost a factor of 1.5–2 for $M \leq 0.3$ GeV, provided we follow the suggestions of Lichard [16], as we have.

In view of the above discussion, we believe that the soft-photon approximation as employed by us is reliable to within a factor of 2. Still it should be certainly worthwhile to have the results of this treatment [18] for the transverse mass distribution to settle this issue, clearly.

B. Low Mass Dileptons

The mechanism for the production of soft virtual photons from bremsstrahlung within a soft photon approximation has been discussed by a number of authors (see Ref. [14] and references therein) in great detail and thus we shall only briefly recall the formulation in order to fix the notation.

The invariant cross-section for the scattering and at the same time production of a soft photon of four momentum $q^\mu = (q^0, \vec{q}) = (E, \vec{q})$ is given by

$$q_0 \frac{d^4\sigma^\gamma}{d^3q dx} = \frac{\alpha}{4\pi^2} \left\{ \sum_{\text{pol}\lambda} J \cdot \epsilon_\lambda \quad J \cdot \epsilon_\lambda \right\} \frac{d\sigma}{dx} \quad (3)$$

where $d\sigma/dx$ is the strong interaction cross-section for the reaction $ab \rightarrow cd$, ϵ_λ is the polarization of the emitted photon, and J^μ is the *virtual photon current* [16] given by

$$J^\mu = -Q_a \frac{2p_a^\mu - q^\mu}{2p_a \cdot q - M^2} - Q_b \frac{2p_b^\mu - q^\mu}{2p_b \cdot q - M^2}$$

$$+ Q_c \frac{2p_c^\mu + q^\mu}{2p_c \cdot q + M^2} + Q_d \frac{2p_d^\mu + q^\mu}{2p_d \cdot q + M^2}. \quad (4)$$

In the above equation the Q 's and p 's represent the charges (in units of proton charge) and the particle four momenta, respectively. The cross-section for the production of dilepton is then obtained as

$$E_+ E_- \frac{d^6\sigma^{e^+e^-}}{d^3p_+ d^3p_-} = \frac{\alpha}{3\pi^2} \frac{1}{q^2} q_0 \frac{d^3\sigma^\gamma}{d^3q} \quad (5)$$

Now the invariant cross-section for dilepton pair production can be written as [14]

$$E_+ E_- \frac{d\sigma_{ab \rightarrow cd}^{e^+e^-}}{d^3p_+ d^3p_-} = \frac{\alpha^2}{12\pi^4 M^2} \int |\epsilon \cdot J|_{ab \rightarrow cd}^2 \frac{d\sigma_{ab \rightarrow cd}}{dt} \times \delta(q^2 - M^2) dM^2 \times \delta^4(q - (p_+ + p_-)) d^4q dt. \quad (6)$$

The rate of production of dileptons at temperature T can then be written as

$$E \frac{dN}{d^4x dM^2 d^3q} = \frac{T^6 g_{ab}}{16\pi^4} \int_{z_{\min}}^{\infty} dz \frac{\lambda(z^2 T^2, m_a^2, m_b^2)}{T^4} \times \Phi(s, s_2, m_a^2, m_b^2) \times K_1(z) E \frac{d\sigma_{ab \rightarrow cd}^{e^+e^-}}{dM^2 d^3q}, \quad (7)$$

where the cross-section for the process $ab \rightarrow cd e^+e^-$ is given by

$$E \frac{d\sigma_{ab \rightarrow cd}^{e^+e^-}}{dM^2 d^3q} = \frac{\alpha^2}{12\pi^3 M^2} \frac{\hat{\sigma}(s)}{E^2}, \quad (8)$$

with

$$\hat{\sigma}(s) = \int_{-\lambda(s, m_a^2, m_b^2)/s}^0 dt \frac{d\sigma_{ab \rightarrow cd}}{dt} \left(q_0^2 |\epsilon \cdot J|_{ab \rightarrow cd}^2 \right), \quad (9)$$

and

$$\Phi(s, s_2, m_a^2, m_b^2) = \frac{\lambda^{1/2}(s_2, m_a^2, m_b^2)}{\lambda^{1/2}(s, m_a^2, m_b^2)} \frac{s}{s_2}, \quad (10)$$

$s_2 = s + M^2 - 2\sqrt{s}q_0$, and $\lambda(x, y, z) = x^2 - 2(y+z)x + (y-z)^2$. The expression for the average of the electromagnetic factor over the solid angle, can be found in Ref. [14]. The value of z_{\min} is obtained from $\lambda(s_2, m_a^2, m_b^2) = 0$. Note that the right hand side of Eq.(8) varies as $1/M^4$ for $\mathbf{q} = 0$.

The strong interaction differential cross-section $d\sigma_{qq}/dt$ and $d\sigma_{qg}/dt$ for scattering of quarks and gluons are obtained from semi-phenomenological expressions used earlier by several authors for this purpose [9,14,15,19]. For hot hadronic matter, we have included the leading reactions: $\pi^+\pi^- \rightarrow \pi^0\pi^0$, $\pi^+\pi^- \rightarrow \pi^+\pi^-$, $\pi^+\pi^0 \rightarrow \pi^+\pi^0$, and $\pi^-\pi^0 \rightarrow \pi^-\pi^0$ and evaluated the strong scattering cross-section from an effective

Lagrangian incorporating σ , ρ , and f meson exchange [9,14,15].

The corresponding expressions for the contribution of annihilation processes $q\bar{q} \rightarrow e^+e^-$ and $\pi^+\pi^- \rightarrow e^+e^-$ are given [20] by,

$$E \frac{dN}{d^4x dM^2 d^3q} = \frac{\sigma_a(M)}{4(2\pi)^5} M^2 e^{-E/T} \left[1 - \frac{4m_a^2}{M^2} \right],$$

$$\sigma_a(M) = F_a \bar{\sigma}(M),$$

$$\bar{\sigma}(M) = \frac{4\pi\alpha^2}{3M^2} \left[1 + \frac{2m_e^2}{M^2} \right] \left[1 - \frac{4m_e^2}{M^2} \right]^{1/2}, \quad (11)$$

where $F_q = 20/3$ for a QGP consisting of u and d quarks, and gluons, and F_π is the pion form factor.

C. Soft Photons

Now we consider soft photon emission through the bremsstrahlung process, $ab \rightarrow cd\gamma$. The invariant cross-section for the above process is obtained from eq. (4) with J^μ replaced by

$$J^\mu = -Q_a \frac{p_a^\mu}{p_a \cdot q} - Q_b \frac{p_b^\mu}{p_b \cdot q} + Q_c \frac{p_c^\mu}{p_c \cdot q} + Q_d \frac{p_d^\mu}{p_d \cdot q}, \quad (12)$$

which is appropriate for the emission of real photons. The rate of production of photons at temperature T can then be written as

$$E \frac{dN}{d^4x d^3q} = \frac{T^6 g_{ab}}{16\pi^4} \int_{z_{\min}}^{\infty} dz \frac{\lambda(z^2 T^2, m_a^2, m_b^2)}{T^4} \times \Phi(s, s_2, m_a^2, m_b^2) K_1(z) E \frac{d\sigma_{ab}^\gamma}{d^3q}, \quad (13)$$

where

$$E \frac{d\sigma_{ab}^\gamma}{d^3q} = \frac{\alpha}{4\pi^2} \frac{\hat{\sigma}(s)}{E^2}, \quad (14)$$

with $\hat{\sigma}(s)$ defined as before (Eq.(9)) with J^μ replaced by real photon current Eq.(12). Even at the risk of repetition, we would like to add that *if we put $M = 0$ in the phase-space factor Φ_2 and use the real photon current in Eq.(7) and Eq.(9)*, we shall have

$$E \frac{dN_{e^+e^-}}{d^4x dM^2 d^3q} \equiv \frac{\alpha}{3\pi M^2} E \frac{dN_\gamma}{d^4x d^3q}, \quad (15)$$

which also remains true in limit $M \rightarrow 0$. Thus a comparison of the expression Eq.(13) with Eq.(7) immediately shows that one may use the results for photons and dileptons (with different masses) with advantage to get information about, say, the evolution of the system.

The annihilation and the Compton processes $q\bar{q} \rightarrow \gamma g$ and $q(\bar{q})g \rightarrow q(\bar{q})g\gamma$ have already been studied in great detail by a number of authors [21]. We only mention the result for a comparison:

$$E \frac{dN_\gamma^{C+ann}}{d^4x d^3q} = \frac{5}{9} \frac{\alpha\alpha_s}{2\pi^2} T^2 e^{-E/T} \ln \left(\frac{2.912ET}{6m_q^2} + 1 \right) \quad (16)$$

where $m_q = \sqrt{2\pi\alpha_s/3}T$ is the thermal mass of the quarks. In the hadronic sector we consider the processes $\pi\rho \rightarrow a_1 \rightarrow \pi\gamma$, $\pi\rho \rightarrow \pi\gamma$ for which rates have been evaluated and parametrized in a convenient form [21–23].

$$E \frac{dN_{\pi\rho \rightarrow a_1 \rightarrow \pi\gamma}}{d^4x d^3q} = 2.4T^{2.15} \exp \left[-1/(1.35TE)^{0.77} - E/T \right], \quad (17)$$

$$E \frac{dN_{\pi\rho \rightarrow \pi\gamma}}{d^4x d^3q} = T^{2.4} \exp \left[-1/(2TE)^{3/4} - E/T \right]. \quad (18)$$

The decay $\omega \rightarrow \pi\gamma$ during the life-time of the interacting system is obtained from,

$$E \frac{dN_{\omega \rightarrow \pi\gamma}}{d^4x d^3q} = \frac{3m_\omega \Gamma_{\omega \rightarrow \pi\gamma}}{16\pi^3 E_0 E} \int_{E_{\min}}^{\infty} dE_\omega E_\omega f_{BE}(E_\omega) \times [1 + f_{BE}(E_\omega - E)] \quad (19)$$

Here $E_{\min} = m_\omega(E^2 + E_0^2)/2EE_0$ and E_0 is the photon energy in the rest frame of the ω meson. Recall that for low energy photons the reactions $\pi\pi \rightarrow \rho\gamma$ and the bremsstrahlung process $\pi\pi \rightarrow \pi\pi\gamma$ are equivalent, and including both of them would amount to a double counting [15,24].

D. Initial Conditions

We have considered central collisions of lead nuclei at CERN SPS, BNL RHIC, and CERN LHC energies. We assume that the collision leads to a thermalized and chemically equilibrated quark gluon plasma at an initial time $\tau_i = 1$ fm/ c and initial temperature T_i . Further assuming an isentropic expansion, one may relate [25] the initial conditions to the multiplicity density (dN/dy);

$$T_i^3 \tau_i = \frac{2\pi^4}{45\zeta(3)\pi R_T^2 4a_k} \frac{dN}{dy}, \quad (20)$$

where R_T is the transverse radius of the lead nucleus and $a_k = 37\pi^2/90$ for a system consisting of massless u and d quarks, and gluons. The evolution of the system is obtained from a boost-invariant longitudinal expansion and cylindrically symmetric transverse expansion [13]. We further assume a first order phase transition to a hadronic matter consisting of π , ρ , ω , and η mesons, ($a_k \approx 4.6\pi^2/90$), at $T = 160$ MeV [26]. After all the quark matter has adiabatically converted to hadronic matter, the system enters a hadronic phase and undergoes a freeze-out at $T = 140$ MeV.

The particle rapidity density is taken as [27] 624, 1735, and 5624 respectively. One may obtain much larger initial temperatures for the same multiplicity densities by

assuming more rapid thermalization of the plasma. An upper limit for this is obtained by taking $\tau_i \simeq 1/3T_i$. We shall argue later, that the multiple scattering effects in the early dense QGP will, however, suppress the soft radiations considerably, and thus the choice of $\tau_i = 1 \text{ fm}/c$ should provide an interesting trade-off between these competing effects.

E. Space-time Integration

The dilepton transverse mass yield is then obtained by convoluting the rates for their emission from QGP and hadronic matter with the space-time history of the system:

$$\frac{dN}{dM^2 d^2 M_T dy} = \int \tau d\tau r dr d\phi d\eta \left[f_Q E \frac{dN^q}{d^4 x dM^2 d^3 q} + (1 - f_Q) E \frac{dN^\pi}{d^4 x dM^2 d^3 q} \right], \quad (21)$$

where $f_Q(r, \tau)$ gives the fraction of the quark matter in the system.

Similarly the photon spectrum is obtained by convoluting the rates for the emission of photons from QGP and the hadronic matter with the space time history of the system;

$$\frac{dN}{d^2 q_T dy} = \int \tau d\tau r dr d\phi d\eta \left[f_Q E \frac{dN^q}{d^4 x d^3 q} + (1 - f_Q) E \frac{dN^\pi}{d^4 x d^3 q} \right]. \quad (22)$$

III. RESULTS

A. Low mass Dileptons

In order to ascertain the relative importance of the contributions of the quark bremsstrahlung, pionic bremsstrahlung, quark annihilation, and pionic annihilation processes to low mass dileptons we show the rates for different values of M at $T = 160 \text{ MeV}$. All the results for the quark annihilation processes are obtained by taking $m_q = 5 \text{ MeV}$. If we adopt the view that $m_q = m_{\text{th}}$, as indeed, we have taken while evaluating the bremsstrahlung contributions, then the quark annihilation contribution will be absent [12] in this mass range. In any case, we see that the quark driven bremsstrahlung processes outshine the pion driven bremsstrahlung contribution (fig.1a-c).

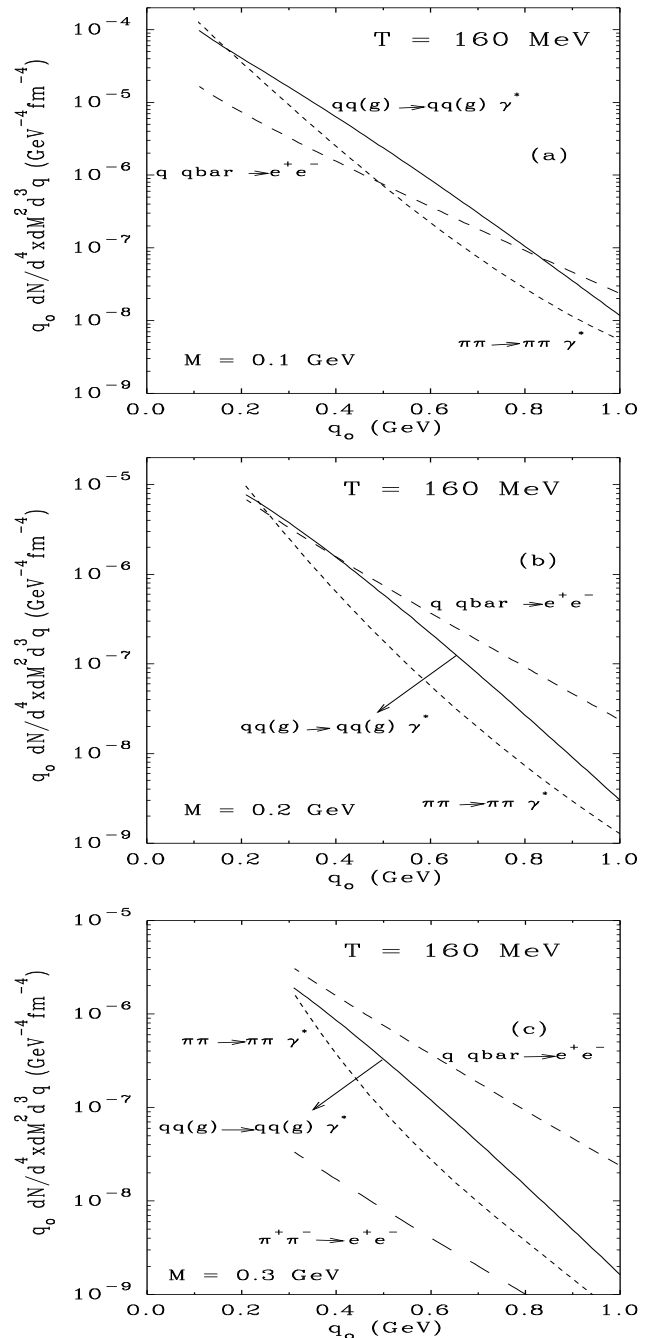


FIG. 1. The production rate of low mass dielectrons from quark and pion bremsstrahlung at $T = 160 \text{ MeV}$. In addition, the contribution of quark annihilation process is given for a comparison. These results are shown for (a) $M = 0.1 \text{ GeV}$, (b) $M = 0.2 \text{ GeV}$, and (c) $M = 0.3 \text{ GeV}$ respectively.

The results for the transverse mass distribution for the low mass dileptons at SPS energies are given in fig.2a-c. We now see that the pion driven processes dominate the yield at all masses as the 4- volume occupied by the hadronic matter is much larger. This is also evident from the invariant mass distribution (fig.2d). Considering that the pion annihilation threshold limits the mass

to $M > 2m_\pi$ and even the quark annihilation may contribute only to masses larger than this, we do find an intense glow of low mass dileptons, once the background from the Dalitz decays of π^0 and η mesons is removed. The recent experience with the CERES experiment [3] has shown that this could be possible to some extent. Recall also that the CERES data for the S+Au system [3] shows a contribution from the bremsstrahlung processes [28]. It will be interesting to find a confirmation of these early observations from the results for the Pb+Pb system as well.

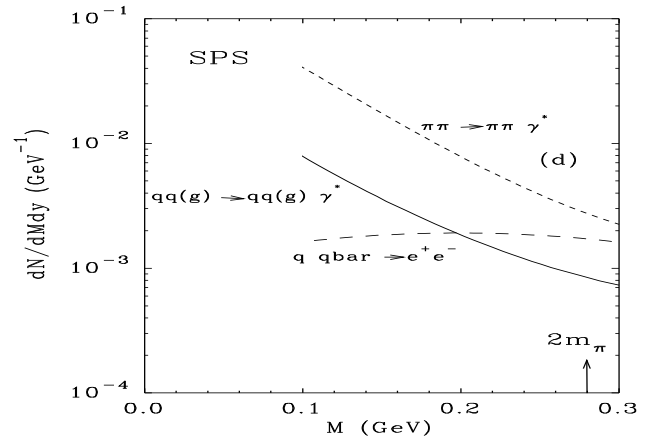
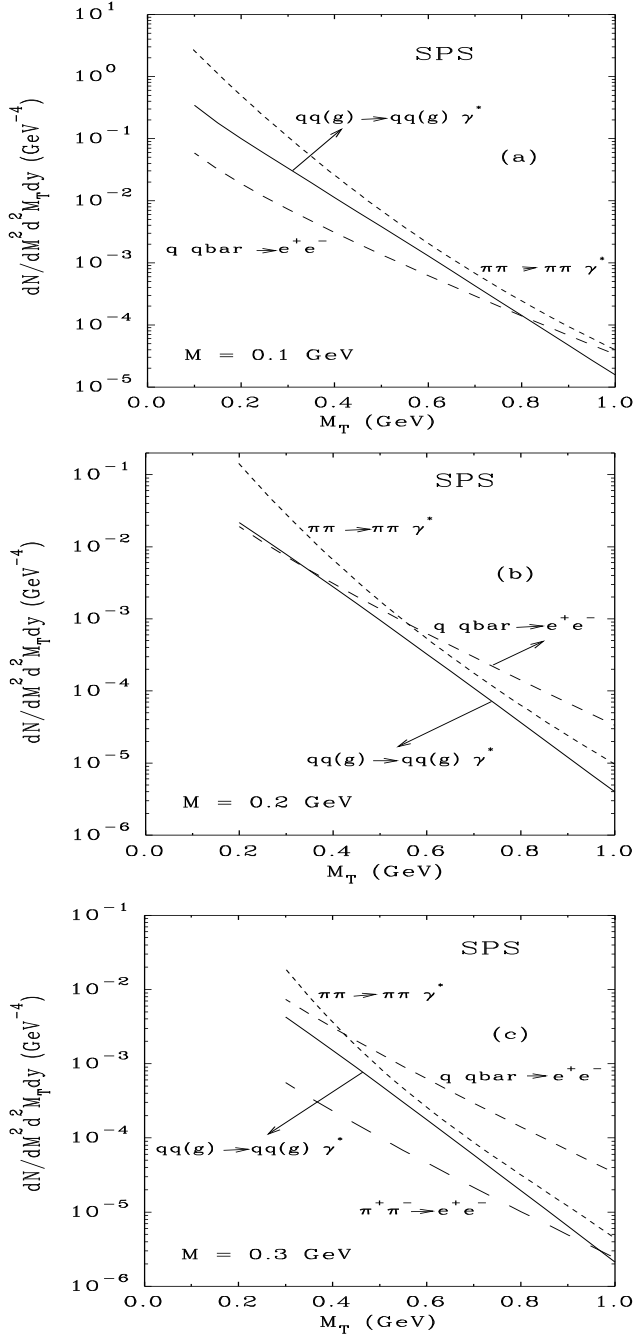
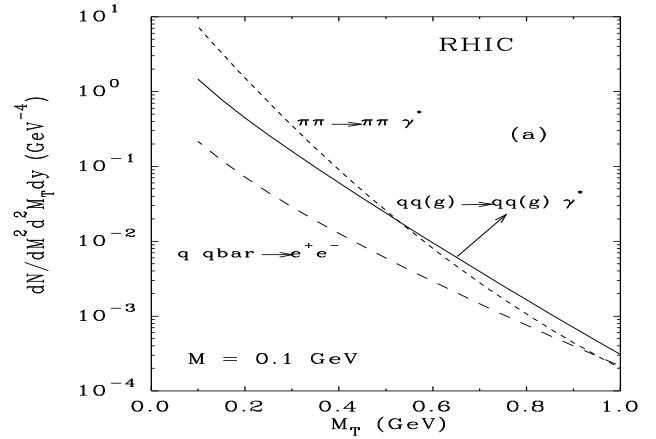


FIG. 2. (a-d): The transverse mass distribution of low mass dielectrons at SPS energies including bremsstrahlung process and annihilation process in the quark matter and the hadronic matter. We give the results for invariant mass M equal to 0.1 GeV (a), 0.2 GeV (b), and 0.3 GeV (c) respectively. The invariant mass distribution of low mass dielectrons are also shown (d).

The transverse mass distribution at RHIC energies (fig.3a-c) reveals another interesting aspect. The transverse mass distribution at lower M_T is dominated by the pion contribution. However at larger M_T , the contributions of the quark driven and pion driven processes are similar. This is a reflection of the larger temperature in the quark phase, and a larger effect of the transverse flow during the hadronic phase. If we look only at the invariant mass distribution (fig.3d), this interesting aspect does not show up.



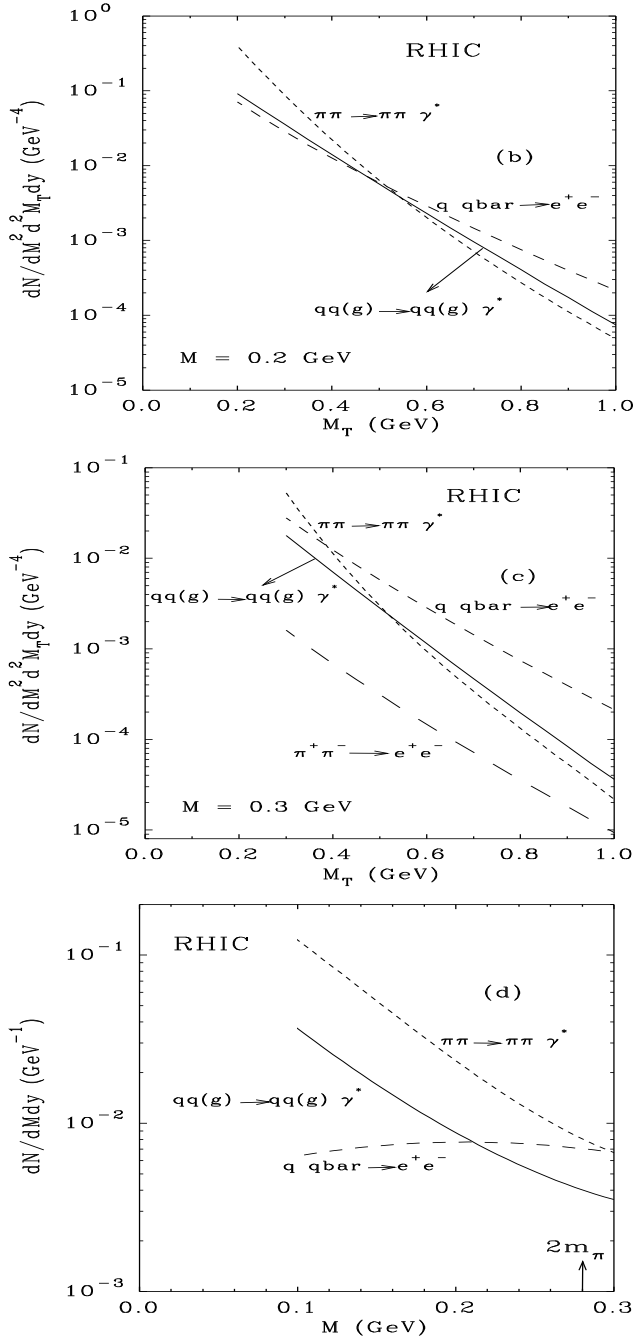


FIG. 3. (a-d): Same as fig. 2, for RHIC energies.

We have further found (not shown here for reasons of space) that, at LHC energies the quark driven bremsstrahlung processes start dominating over the pion driven bremsstrahlung processes even at relatively smaller M_T , as the slopes of the quark-driven processes are much smaller. This aspect remains true even in the invariant mass spectrum, and the contributions become similar at $M = 0.3$ GeV.

These results also clearly reveal the rapidly changing importance of the different processes considered here leading to low mass dileptons, as the available energy

(initial conditions) changes and as the invariant mass M assumes varying values. When detailed results are available these considerations may help resolve different contributions.

We envisage an increase by a factor of 2–4 in the dilepton yield as we go from SPS to RHIC energies, and by a factor of 15–20 as we go from SPS to LHC energies. Thus the existence of a longlived interacting system would be characterized by an intense glow of low mass dileptons. This means a large increase in the electromagnetic signals, as compared to the estimates done by using only pion and quark annihilations.

It is well known that ratios of particle spectra can sensitively reveal the details of the variations of the underlying processes. We have seen in Eq.(8) that the transverse mass-spectra for low mass dileptons are proportional to $1/M^2$. In figs.4–6 we have plotted the ratio of $M^2 dN/d^2M_T dM^2 dy$ at $M = 0.1$ GeV to that for $M = 0.2$ GeV and $M = 0.3$ GeV both with (solid line) and without (dashed line) the transverse flow at SPS, RHIC, and LHC respectively. We have verified that the (oscillatory) structure seen in the results without the transverse flow has its origin in the structure in $\pi\pi$ scattering cross-section, which is sampled in the process. One can also show that if there is no transverse expansion of the system then the ratios as depicted here would be independent of the initial temperature, that is they would be identical for SPS, RHIC, and LHC energies, which is also seen from these figures. A deviation from this universal behaviour is indicative of the increasing importance of the transverse flow as one increases the initial temperature of the system, which in turn decides the overall life-time of the system.

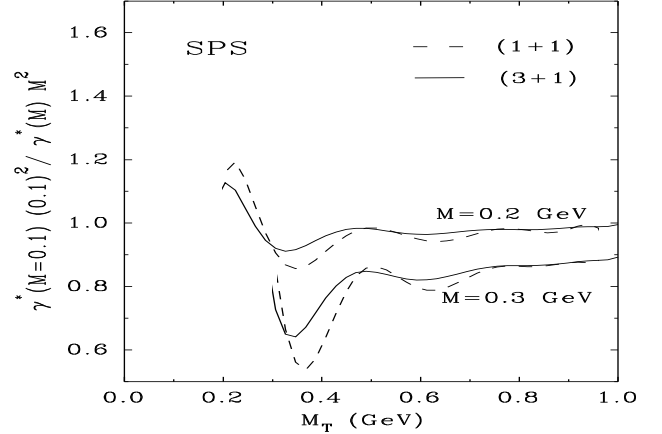


FIG. 4. The ratio of M^2 weighted differential dielectron yield $M^2 dN/dM^2 d^2M_T dy$ at $M = 0.1$ GeV to that at $M = 0.2$ GeV and $M = 0.3$ GeV as a function of transverse mass M_T for SPS energies. The solid curve gives the total contribution (quark matter + hadronic matter) with the transverse flow. Similarly the dashed curve gives the total contribution without the transverse flow.

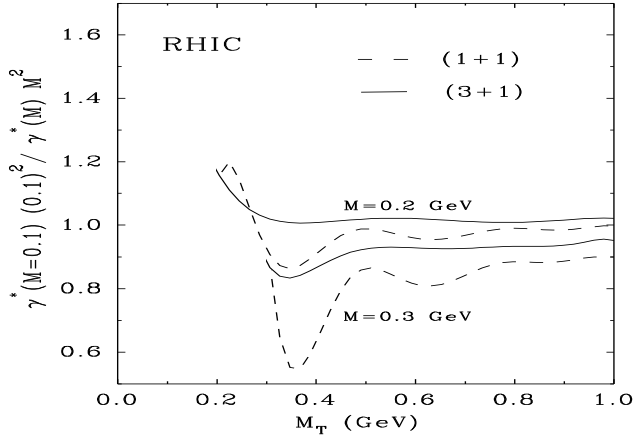


FIG. 5. Same as fig. 4 for RHIC energies. The definition of the solid and the dashed curves are same as in fig. 4.

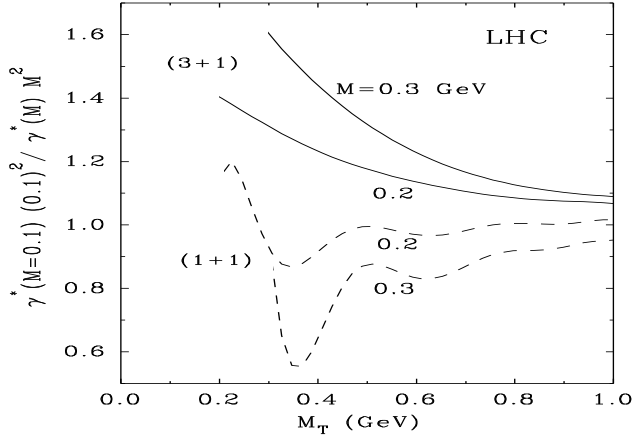


FIG. 6. Same as fig. 4 for LHC energies. The definition of the solid and the dashed curves are same as in fig. 4.

Finally, while investigating the dependence of our results on the freeze-out temperature a successively increasing dependence on this last stage of the interacting system was seen as we go from SPS to RHIC to LHC energies. The largest sensitivity is thus seen for the LHC energies (see fig. 7), where the life-time of the interacting system is longest, giving the transverse flow effects ample scope to come into full play.

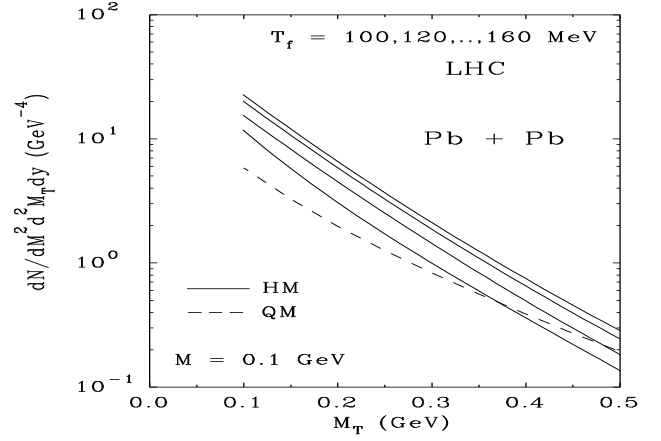


FIG. 7. Sensitivity of the low mass dielectron spectra to the freeze-out temperature at LHC energies for $M = 0.1$ GeV.

B. Soft Photons

In a manner similar to the above, we have plotted the rates for different photon producing processes at $T = 160$ MeV (fig.8). We see that the quark and pion driven bremsstrahlung processes dominate upto energies of a few hundred MeV, after which they fall rapidly.

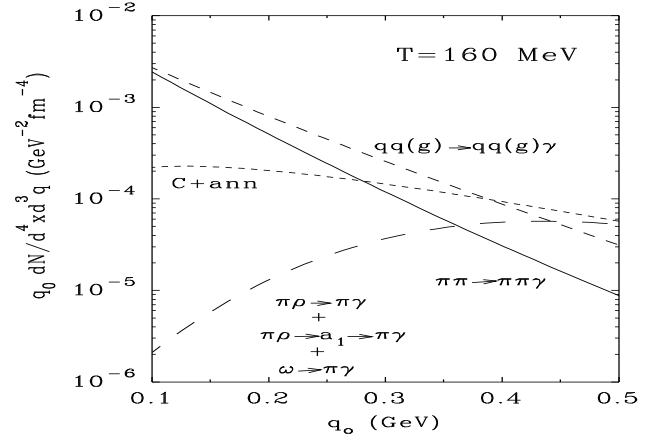


FIG. 8. Soft photon production rate at $T = 160$ MeV from quark and pion bremsstrahlung, Compton + annihilation processes and the sum of the main hadronic reactions as shown in the figure.

Space-time integrated results for RHIC energies are shown in fig.9. We find that soft photons having transverse momenta of upto a few hundred MeV mostly originate from pion driven bremsstrahlung processes, and once again the existence of a longlived interacting system is revealed by an intense glow of soft photons, once the background of decay photons is removed.

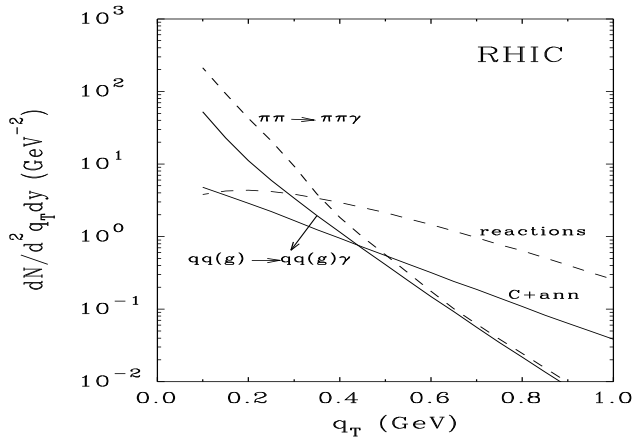


FIG. 9. The transverse momentum distribution of soft photons from different mechanisms at RHIC energies. The sum of the contribution $\pi\rho \rightarrow \pi\gamma$, $\pi\rho \rightarrow a_1 \rightarrow \pi\gamma$ and the decay $\omega \rightarrow \pi\gamma$ is referred as 'reactions'.

Even though the relative importance of the various contributions was found to be similar at SPS and LHC energies, we envisage an increase by a factor of 2–4 in the yield of photons having $p_T = 200$ MeV, as we go from SPS to RHIC and an increase by a factor of almost 10 as we go from SPS to LHC energies. The complete dominance of soft photons in determining the multiplicity of photons produced is seen from fig.10. Note that we have included only photons having $p_T > 100$ MeV, for this discussion, as we know that the yield for lower p_T is subject to Landau Pomeranchuk effect. It may be noted, however, that unlike the case of dileptons, the contribution of the reaction $\pi\pi \rightarrow \rho\gamma$ which is equivalent to $\pi\pi \rightarrow \pi\pi\gamma$ was included in the estimates of single photons [21], and thus the increase above does not necessarily mean a new source. It merely points to a rapid rise in the yield of single photons having $p_T < 300$ –400 MeV.

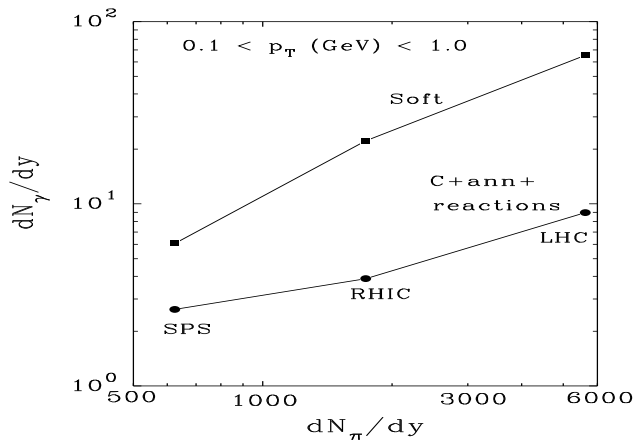


FIG. 10. Soft photons vs. photons from Compton plus annihilation processes from the QGP and hadronic reactions at SPS, RHIC, and LHC energies from central collision of two lead nuclei.

IV. DISCUSSION

There are a number of aspects which should be discussed before we draw our conclusions. We have already discussed the validity of the soft-photon approximation in sect. II.

It is well-known that bremsstrahlung radiation could be very large for light particles and one may worry about this aspect for the radiations from the quark matter. We have, however, used the thermal mass of quarks while evaluating the $d\sigma/dt$ as well as the kinematics of the collision, which is appropriate for fermions moving in a hot medium. We have already stated that if we extend this argument to quark annihilation as well, then the bremsstrahlung processes become the leading contributors to this mass range for dileptons.

Any study of soft electromagnetic radiations must address the question of Landau-Pomeranchuk [29] suppression of such processes in a dense medium. The Landau-Pomeranchuk effect provides that if the formation time of a particle is more than the time between two collisions, the emission of the particle could be considerably suppressed due to destructive interference of multiple scatterings. We would like to draw the attention of the readers to arguments developed in Ref. [15] earlier, about the extent of the modifications to our predictions due to this. It can be argued that our results for the sum of the radiations from the interacting system will remain fairly free from the effects of Landau-Pomeranchuk suppression till we restrict ourselves to photons and dileptons having energies larger than a few hundred MeV. The Landau-Pomeranchuk suppression could be severe for lower energies as, indeed, demonstrated by Cleymans et al. [30].

These considerations have an interesting connotation. Recall that we have taken the initial time as 1 fm/c. It is quite likely that the QGP may be thermalized much more quickly [27], and then we can have a larger initial temperature for the same multiplicity of the particles. We have seen earlier that the partonic density can then be much higher, and thus there would be a suppression of soft radiations. Thus our choice of $\tau_i = 1$ fm/c ensures that we start our evaluations *after* the Landau-Pomeranchuk effect has lost its dominating effect, and that our estimates remain reasonable. A more complete treatment will include the Landau Pomeranchuk effect and thus these suppressions would be automatically, and more properly accounted for.

We have approximated the hadronic phase as a non-interacting gas of π , ρ , ω , and η mesons. How will the results differ for a richer hadronic matter, which would result in a reduced life-time for the mixed-phase? A richer equation of state for hadronic matter will also imply a smaller speed of sound, and the attendant slower cooling of the system, and a longer life time for the hadronic phase. Thus, it was found recently that the results for single photons [31] with a truncated equation of state as

used here and a resonance gas containing all hadrons, for the hadronic matter left the final results essentially unaltered. Similar results should be expected here, due to the similarity of the rates for the quark and pion driven processes (see. fig.1).

All our evaluations are made with the assumption that the QGP, as produced initially, is in kinetic and chemical equilibrium, and that its evolution is isentropic. It is quite likely that the plasma as produced in relativistic heavy ion collisions is neither in kinetic nor in chemical equilibrium. How will this affect our findings? Even though the kinetic equilibrium could be achieved quickly enough, the chemical equilibration itself may not be achieved at all [32–34]. The contributions of the QGP part is then easily obtained by introducing the products $\lambda_i \lambda_j$, where λ_i is the fugacity of the parton species i , in our expressions [35]. Needless to add that the overall contribution could come down by a factor of upto 10 or more depending upon the initial conditions. So far there is no treatment which could model the hadronization of QGP which is far from chemical equilibrium. It is not even clear that such a matter will go through a mixed phase. The description of the hadronic phase (if any) also gets uncertain. However, a very interesting outcome of this scenario could be a complete absence of radiations from the hadronic processes, if the QGP phase is not followed by an interacting hadronic matter living for some finite time! This could be of great interest.

What could be other sources of low mass dileptons? It was suggested some time ago [28] that $\pi\rho \rightarrow \pi e^+e^-$ could contribute to low mass dileptons. This has now been evaluated [7], and it is found to contribute less than the bremsstrahlung processes at lower masses. However the bremsstrahlung contribution decreases rapidly and for $M > 300$ MeV, and the above reaction contributes at a level of 10–50% of the pionic annihilation. It will be of interest to study the transverse mass distribution of this reaction, as it is likely to be different.

V. SUMMARY

We have calculated the transverse mass distribution of low mass dileptons and transverse momentum distribution of soft photons from central collision of two lead nuclei at CERN SPS, BNL RHIC, and CERN LHC energies. We assume that the collision leads to a thermalized and chemically equilibrated quark gluon plasma at the proper time $\tau_i = 1$ fm/c. The plasma then expands, cools, and gets into a mixed phase at $T = 160$ MeV. After all the quark matter is adiabatically converted to hadronic matter, it cools again, and undergoes a freeze-out at $T = 140$ MeV. We have considered a boost invariant longitudinal and cylindrically symmetric transverse expansion. This is, to our knowledge, the first treatment of the dynamics of soft electromagnetic radiations in such collisions, with transverse expansion, whose effect is seen to be large

when the life-time of the interacting system is large.

We find that the formation of such a system may be characterized by an intense glow of soft electromagnetic radiations, whose features depend sensitively on the last stage of evolution, once we remove the background of decay photons or dileptons.

We are grateful to Hans Eggers and Kevin Haglin for very many useful discussions during the course of this work.

-
- [1] R. Rckl, Phys. Lett. B**64**, 39 (1976).
 - [2] G. Q. Li, C. M. Ko, and G. E. Brown, Phys. Rev. Lett. **75**, 4007 (1995).
 - [3] G. Agakichiev et al., CERES Collaboration, Phys. Rev. Lett. **75**, 1272 (1995).
 - [4] C. M. Ko, Talk given at Quark Matter '96, and to be published.
 - [5] J. Gaber and H. Leutwyler, Phys. Lett. B **184**, 83 (1987).
 - [6] R. D. Pisarski, Nucl. Phys. A **590**, 553c (1995).
 - [7] K. Haglin, Phys. Rev. C**53**, R2606 (1996).
 - [8] J. Cleymans, K. Redlich, and H. Satz, Z. Phys. C**53**, 517 (1991).
 - [9] K. Haglin, C. Gale, and V. Emel'yanov, Phys. Rev. D**47**, 973 (1993).
 - [10] E. Braaten and R. D. Pisarski, Nucl. Phys. B **337**, 569(1990).
 - [11] H. A. Weldon, Phys. Rev. Lett. **66**, 293 (1991).
 - [12] A. Peshier, B. Kmpfer, O. P. Pavlenko, and G. Soff, Phys. Lett. B **337**, 235 (1994).
 - [13] H. von Gersdorff, L. McLerran, M. Kataja, and P. V. Ruuskanen, Phys. Rev. D **34**, 794 (1986).
 - [14] D. Pal, K. Haglin, and D. K. Srivastava, Phys. Rev. C **54**, 1366 (1996).
 - [15] P. K. Roy, D. Pal, S. Sarkar, D. K. Srivastava, and B. Sinha, Phys. Rev. C **53**, 2367 (1996).
 - [16] P. Lichard, Phys. Rev. D **51**, 6107 (1995).
 - [17] E. Braaten, R. D. Pisarski, and T. C. Yuan, Phys. Rev. Lett. **64**, 2242 (1990).
 - [18] H. C. Eggers, R. Tabti, C. Gale, and K. Haglin, Phys. Rev. D **53**, 4822 (1996).
 - [19] P. Danielewicz and M. Gyulassy, Phys. Rev. D **31**, 53 (1985).
 - [20] K. Kajantie, J. Kapusta, L. McLerran, and A. Mekjian, Phys. Rev. D **34**, 2746 (1986).
 - [21] J. Kapusta, P. Lichard, and D. Seibert, Phys. Rev. D **44**, 2774 (1991).
 - [22] L. Xiong, E. Shuryak, and G. E. Brown, Phys. Rev. D **46**, 3798 (1992).
 - [23] H. Nadeau and J. Kapusta, Phys. Rev. C **45**, 3034 (1992).
 - [24] V. V. Goloviznin and K. Redlich, Phys. Lett. B **319**, 520 (1993).
 - [25] R. C. Hwa and K. Kajantie, Phys. Rev. D **32**, 1109 (1985).
 - [26] J. Alam, D. K. Srivastava, B. Sinha, and D. N. Basu, Phys. Rev. D **48**, 1117 (1993).

- [27] J. Kapusta, L. D. McLerran, and D. K. Srivastava, Phys. Lett. B **283**, 145 (1992).
- [28] D. K. Srivastava, B. Sinha, and C. Gale, Phys. Rev. C **53**, R567 (1996).
- [29] L. Landau and I. Pomeranchuk, Dokl. Akad. Nauk. SSSR **92**, 535 (1953), *ibid.* **92**, 735 (1953); A. B. Migdal, Phys. Rev. **103**, 429 (1956).
- [30] J. Cleymans, V. V. Goloviznin, and K. Redlich, Phys. Rev. D **47**, 989 (1993);
- [31] J. Cleymans, K. Redlich, and D. K. Srivastava, GSI-Preprint-96-42, and submitted to Phys. Rev. C.
- [32] K. Geiger, Phys. Rep. **258**, 376 (1995).
- [33] T. S. Biro, E. von Doorn, B. Müller, M. H. Thoma, and X. N. Wang, Phys. Rev. C **48**, 1275 (1993).
- [34] D. K. Srivastava, M. G. Mustafa, and B. Müller, <hep-ph/9608424 >.
- [35] M. T. Strickland, Phys. Lett. B **331**, 245 (1994).

FIGURE CAPTIONS

Figure (1a-c): The production rate of low mass dielectrons from quark and pion bremsstrahlung at $T = 160$ MeV. In addition, the contribution of quark annihilation process is given for a comparison. These results are shown for (a) $M = 0.1$ GeV, (b) $M = 0.2$ GeV, and (c) $M = 0.3$ GeV respectively.

Figure (2a-d): The transverse mass distribution of low mass dielectrons at SPS energies including bremsstrahlung process and annihilation process in the quark matter and the hadronic matter. We give the results for invariant mass M equal to 0.1 GeV (a), 0.2 GeV (b), and 0.3 GeV (c) respectively. The invariant mass distribution of low mass dielectrons are also shown (d).

Figure (3a-d): Same as fig. 2, for RHIC energies.

Figure 4: The ratio of M^2 weighted differential dielectron yield $M^2 dN/dM^2 d^2M_T dy$ at $M = 0.1$ GeV to that at $M = 0.2$ GeV and $M = 0.3$ GeV as a function of transverse mass M_T . The solid curve gives the total contribution (quark matter + hadronic matter) with the transverse flow. Similarly the dashed curve gives the total contribution without the transverse flow.

Figure 5: Same as fig. 4 for RHIC energies. The definition of the solid and the dashed curves are same as in fig. 4.

Figure 6: Same as fig. 4 for LHC energies. The definition of the solid and the dashed curves are same as in fig. 4.

Figure 7: Sensitivity of the low mass dielectron spec-

tra to the freeze-out temperature at LHC energies for $M = 0.1$ GeV.

Figure 8: Soft photon production rate at $T = 160$ MeV from quark and pion bremsstrahlung, Compton + annihilation processes and the sum of the main hadronic reactions as shown in the figure.

Figure 9: The transverse momentum distribution of soft photons from different mechanisms at RHIC energies. The sum of the contribution $\pi\rho \rightarrow \pi\gamma$, $\pi\rho \rightarrow a_1 \rightarrow \pi\gamma$ and the decay $\omega \rightarrow \pi\gamma$ is referred as 'reactions'.

Figure 10: Soft photons vs. photons from Compton plus annihilation processes from the QGP and hadronic reactions at SPS, RHIC, and LHC energies from central collision of two lead nuclei.